FATIGUE CRACK GROWTH OF TWO X52 PIPELINE STEELS IN A PRESSURIZED HYDROGEN ENVIRONMENT*

A.J. SLIFKA
NIST, Materials Reliability Division
325 Broadway
Boulder, CO 80305 USA

E.S. DREXLER
NIST, Materials Reliability Division
325 Broadway
Boulder, CO 80305 USA

N. RUSTAGI
NIST, Materials Reliability Division
325 Broadway
Boulder, CO 80305 USA

D.S. LAURIA
NIST, Materials Reliability Division
325 Broadway
Boulder, CO 80305 USA

J.D. MCCCOLSKEY
NIST, Materials Reliability Division
325 Broadway
Boulder, CO 80305 USA

R.L. AMARO
NIST, Materials Reliability Division
325 Broadway
Boulder, CO 80305 USA

A.E. STEVENSON
NIST, Materials Reliability Division
325 Broadway
Boulder, CO 80305 USA

P.G. KEEFE
NIST, Materials Reliability Division
325 Broadway
Boulder, CO 80305 USA

ABSTRACT

Fatigue crack growth tests were conducted on two API 5L X52 pipeline steel alloys. One alloy was from a new pipe that was installed for hydrogen service in 2011. The other alloy was from a vintage pipe that first saw natural gas service in 1964. Baseline tests were conducted in air, and those results were compared with tests conducted in pressurized hydrogen gas. All tests were run at (load ratio) R = 0.5 and a frequency of 1 Hz. Tests were conducted at hydrogen pressures of 5.5 MPa and 34 MPa. A new method that tests 10 compact tension specimens simultaneously for fatigue crack growth rate (FCGR) was used, and is briefly described. Fatigue crack growth rates for both alloys were significantly higher in a pressurized hydrogen environment than in air.

INTRODUCTION

The emphasis on research in the area of clean energy must include hydrogen, based on it being the cleanest burning combustible fuel. Hydrogen is also an excellent energy carrier, such that if renewable sources of energy can be used to electrolyze water to generate hydrogen and if the transport of hydrogen fuel can be accomplished efficiently, our nation could greatly reduce reliance on foreign sources of fuel. Renewable sources such as wind and solar are frequently producing energy at times when it is not being used; this excess energy can be

used for hydrogen production. Safe, reliable, efficient transport of hydrogen is needed, and pipelines have been shown to be the best solution for fuels. Additionally, vehicles that run on hydrogen by way of fuel cells are still planned to be available from commercial suppliers such as Mercedes-Benz, Honda, Hyundai, and Toyota by 2015 [1, 2]. The U.S. is falling behind Korea and Japan in hydrogen technology at a time when one would think that, based on energy usage and demand, the U.S. would be the world leader in alternative energies [3].

An issue with fatigue testing of steels in hydrogen gas is that the tests need to be performed at low cyclic frequencies in order to give the hydrogen time to adsorb on the surface, dissociate, and diffuse to the crack tip. This provides the maximum potential detrimental effect of hydrogen (if the effect of temperature is ignored) such that a conservative lifetime of a pipeline can be determined. In order to obtain FCGR data in a more timely fashion, NIST has developed a linked system where 10 specimens can be simultaneously tested in a pressurized gas environment. The specimens remain in the test vessel at pressure until the last of the 10 specimens has completed the FCGR test. As far as the authors know, this is the first time multiple specimens have been tested for FCGR in a pressurized gas environment where all specimens complete the test before the chamber is opened.

Most recent research on pipeline steels has been done on hydrogen-induced cracking, which used cathodic charging [4-7]. However, there has also been recent work on fatigue of pipeline steels, although the literature includes both work on pipeline steels and a range of other alloys [8-15]. New pipelines in the U.S. intended for hydrogen service are currently X52 steel, based on the ASME B31.12 code on Hydrogen Piping and Pipelines [16]. Higher-strength alloys are given a penalty for potential hydrogen embrittlement, based on tensile-test results from the historic literature. The lack of fatigue data on API 5L steel alloys in the X-series makes this penalty necessary. It is possible that this conservatism can be relaxed if future fatigue measurements on higher-strength alloys show that hydrogen embrittlement in the case of dynamic loading is not as severe as in the case of monotonic loading. This current research will provide a baseline for FCGR of new (2011) X52 steel alloy, and a comparison will be made in this research with a vintage X52 pipeline material that was placed in natural gas service in 1964. It is possible that vintage, lower-strength steels could be re-purposed for hydrogen service if FCGR data could be generated for microstructures typical of older alloys and suitable models could generate lifetime predictions.

MATERIALS

Two X52 steel alloys were obtained from commercial gas companies. One material had not seen service, and was extracted from material that had been manufactured specifically for a hydrogen pipeline that was installed in the U.S. in 2011. This material had very low carbon content to enhance weldability, and was microalloyed. The pipe was 508 mm (20 in.) in diameter and had a wall thickness of 10.6 mm (0.423 in.). The other material had been taken out of natural gas service at an unknown time, but was put into service in 1964. The

vintage pipe was 914 mm (36 in.) diameter with a 10.6 mm (0.423 in.) wall thickness. Both pipes were made from rolled plate material with long seams welded in the longitudinal direction. Therefore the rolling direction of the material was the pipe longitudinal direction. Table 1 shows the chemical analyses of the two alloys. Note that the vintage steel has much higher carbon content. The vintage steel had a polygonal ferrite-pearlite microstructure, shown in Fig.1a.The microstructure of the new alloy is shown in Fig. 1b. This material contains a mixture of polygonal ferrite, acicular ferrite and dispersed carbides with a fine, homogeneous grain structure. Neither of the two steels shows banding due to chemical microsegregation at low magnification.

Compact tension (C(T)) specimens were machined from the pipes to a size of w=44.5 mm, which is the largest size that our hydrogen tests vessels can accommodate. The specimens were made and tested in accordance with ASTM E647-05 [17]. Since many were to be tested in pressurized hydrogen gas, they were polished to a fine surface finish, <250 nm, in accordance with ASTM G142-98 [18]. Tensile properties in the transverse pipe direction for the two steels can be seen in Table 2. The vintage alloy does not technically qualify as X52 according to our recent tensile tests of four specimens of that material. All tensile tests were done in air and in accordance with ASTM E-08 [19]. Baseline FCGR tests in air were done on each alloy, as well as tests in 5.5 MPa and 34 MPa hydrogen gas.

a. 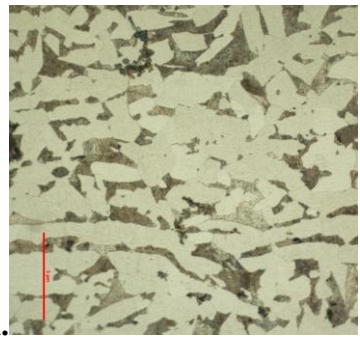 **b.** 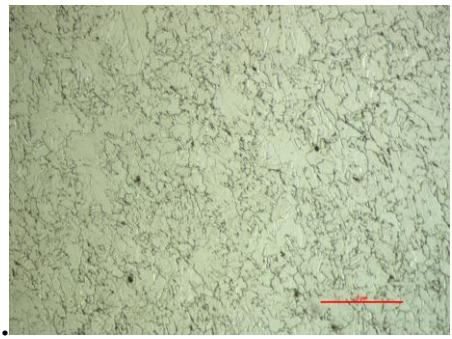

Figure 1. (a)Ferrite-pearlite microstructure of the vintage alloy, where the rolling direction is horizontal (pipe longitudinal direction). (b)Microstructure of the new X52 alloy. The scale bars are 5 micrometers.

Table 1. Chemistries of the two X52 alloys.

	C	Mn	Si	P	S	Al	Cr
X52_vintage	0.238	0.96	0.064	0.011	0.021	0.002	0.014
X52_new	0.071	1.06	0.24	0.012	0.004	0.017	0.033
	Ni	Mo	Nb	Ti	V	Cu	
X52_vintage	0.003	0.004	0.001	0.002	0.002	0.085	
X52_new	0.004	0.003	0.026	0.038	0.004	0.016	

Table 2. Tensile properties of the two X52 alloys.

Steel	σ_y [MPa, mean ± std. dev.]	σ_{UTS} [MPa, mean ± std. dev.]
X52_vintage	325±4	526±4
X52_new	487±5	588±5

METHOD

FCGR tests were done in accordance with ASTM E647 in atmospheric air and pressurized hydrogen gas [17]. Instead of testing one specimen at a time, a new method for simultaneously testing 10 specimens was used. The system used to produce and maintain hydrogen pressure and the linked-specimen system are briefly described below.

Gas Pressurization System

A 316 stainless steel pressure vessel, capable of 34 MPa, that had an internal diameter of 127 mm and an internal length of 813 mm was used to contain the set of 10 specimens used in each set of tests for this work. After installation of the set of 10 specimens into the test vessel, three purges with ultra-pure helium (99.9999 %) and three purges with ultra-pure hydrogen (99.9995 %) are used to clean the chamber. The fourth fill with ultra-pure hydrogen is used as the test gas. The first two helium purges are done at 14 MPa, followed by a purge at the test gas pressure. The three hydrogen purges are done at 14 MPa, followed by the final hydrogen fill at the test pressure. The typical concentrations of oxygen and water in the hydrogen gas sampled following a test is less than 0.5 ppm and less than 1 ppm, respectively. An automated system that uses a program written in-house at NIST performs these purges and keeps the test vessel within 3 % of the target test pressure for the duration of the test. The automation allows these tests to continue 24 hours a day, 7 days a week until all 10 specimens have run their respective cracks out to a length of 0.75*w*, where *w* is the length of a specimen along the crack path from the load line to the edge [17].

Linked-Specimen System

The specimens were linked together such that each specimen cracks a preset amount, but no further, before any specimen completely fractures. The chamber must remain under pressure until all specimens have cracked to a length of about 0.75*w*, so the links, attached to the outside of the clevises, bear the load of the completed specimens prior to complete fracture. Figure 2 shows a link and a schematic drawing of the elongated hole that is sized so that the final crack length is about 0.75*w*, slightly longer than the length that can be used for valid FCGR data in ASTM E647.

The linked system is assembled with the specimens, clevises, links, and polytetrafluoroethylene (PTFE) spacers between the specimens and clevises. Aluminum spacers that set between clevises have thicknesses that make the set of specimens, clevises, and links stand straight for insertion into the test chamber. Since the tests are run at a load ratio of 0.5, the linked system only experiences tension; therefore, once the chain of specimens is loaded in tension, the spacers play no further role. Figure 3 shows a portion of the set of 10

specimens, with the clevises, links, and aluminum spacers noted. The set of 10 specimens is tested in load control. An internal load cell, mounted at the bottom of the set of specimens, is used inside the chamber for load measurement and control. The load cell is a custom design that uses strain gages. Care must be taken that the chamber is not de-pressurized at more than 69 kPa per minute. Faster de-pressurization can result in damage to the strain gages. Measurements over the past two years have shown drift in the load cell of less than 2 % during that time. However, the load cell is re-calibrated at least 4 times per year.

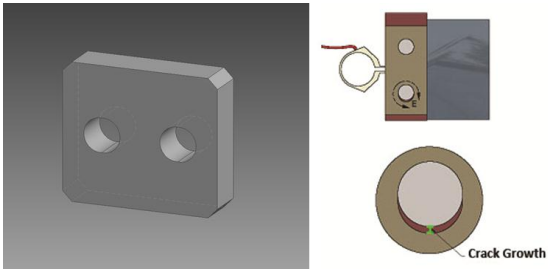

Figure 2. Schematic drawing of the link, left, and the elongated hole, right, that allows crack extension but precludes specimen failure.

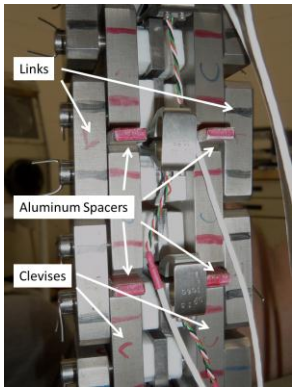

Figure 3. A portion of the linked-specimen system, showing two specimens and the component features of the system.

RESULTS

A set of 10 specimens that consisted of three thicknesses of each of the new and vintage X52 alloys was run in air at 1 Hz loading frequency. A second, similar set was installed inside the chamber and tested at 5.5 MPa hydrogen gas and 1 Hz loading frequency. Different thicknesses were used in order to more efficiently populate the FCGR curve. A calculation can be used to determine the thickness needed for a specimen of a given material to provide a desired starting ΔK. Although all of the specimens of a given alloy were cut from the same pipe, and all from the 2 o'clock position (where the 12 o'clock position is the seam weld), and were tested at the same time, in the same environment, they do not perfectly overlay each other. However, the range of the data at a given ΔK provides an estimate of the measurement uncertainty. Some of the data range comes from overlapping data, due to specimens of different thickness, and some from the fact that we include repeat samples.

For the set of data on both the new and vintage X52 materials measured in hydrogen, we started with a string of 10 specimens, where each alloy had one thin, one medium, two thick, and a weld specimen included. The weld specimens were a girth weld for the vintage material and a seam weld for the new material, where the crack is always oriented along the weld. The new X52

material used electrical resistance welding (ERW) for the seam welds and shielded gas metal arc welding (SMAW) for the girth welds. The vintage material had submerged arc welding (SAW) seam welds and used SMAW for the girth welds. These were included for a preliminary indication of whether the FCGR for welds was significantly different than base metal for these two X52 alloys, but data for these will not be included in this work. To verify the concept of the linked specimens, this first test in hydrogen was run for a short time, until one thin and one medium thickness specimen cracked, then halted. The chamber was removed and the linked set of specimens and crack mouth opening displacement (CMOD) gauges inspected. The CMOD gauges are also strain-gauge devices, similar to the internal load cell. Therefore, they also must experience de-pressurization of less than 69 kPa per minute. The calibration of all ten CMOD gauges is checked before every set of specimens is tested. The system worked as intended, so those 4 specimens that had cracked were replaced with new specimens of similar thicknesses and that set was run to completion of all 10 specimens. Figure 4 shows the FCGR curves for both the new and vintage materials in both air and 5.5 MPa hydrogen gas, loaded at 1 Hz and R=0.5. The air tests from both new and vintage materials are presented in one color because there is no difference in air between the two alloys. For comparison, FCGR data is added from Sandia National Laboratories (SNL), shown for hydrogen at 21 MPa, R=0.5, and 1 Hz as a solid line, and for air at R=0.5, and 10 Hz as a dashed line [20]. The X52 alloy that they studied had a microstructure consisting of 10 % pearlite in a polygonal ferrite matrix from a linepipe of 1990s vintage with carbon and manganese contents of 0.06 % and 0.87 %, respectively.

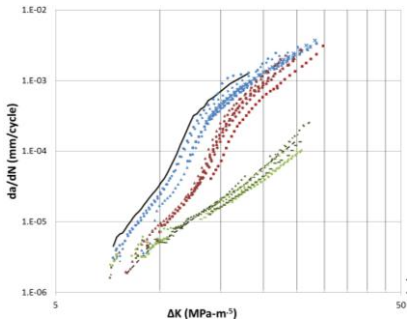

Figure 4. Comparison of FCGR data in air (green) and in 5.5 MPa hydrogen gas for two X52 alloys at 1 Hz loading frequency (blue, new X52 and red, old X52)and R=0.5. Data from Sandia National Laboratories (SNL) added for comparison (lines)[19].

DISCUSSION

The air data from both X52 alloys show no significant difference in Fig. 4. Running the same alloys in 5.5 MPa hydrogen resulted in much higher FCGRs, except at the lowest ΔKs. The scatter of the hydrogen data is similar to the scatter of the air data for both alloys. At ΔK=15 MPa·m$^{1/2}$, the average

uncertainty is $1x10^{-4}$ mm/cycle. The data in Fig. 4 appear to show that the vintage alloy outperforms the new alloy. There is some overlap between the new and vintage material data sets, and they appear to converge at high ΔK. A statistical analysis would have to be undertaken to determine whether there is indeed a significant difference, and what that statistical significance was. From a metallurgical standpoint, the newer, cleaner steel might be expected to perform better, but perhaps the large ferrite grain size of the older material provides slower hydrogen diffusion [21, 22]. Finer grain-sized material with more grain boundaries could enhance diffusion, although the traps from microalloying elements could retard diffusion.

At low ΔKs the increase in FCGR is very rapid, probably due to increased hydrogen concentration at the crack tip due to stress-enhanced diffusion [23]. This appears to continue until the "knee" in the curve is reached, which occurs at around 13 MPa·$m^{1/2}$ for the new alloy and around 15 MPa·$m^{1/2}$ for the vintage steel. Beyond this point, at increasing ΔKs, the slope of the FCGR curves in hydrogen are approximately the same as those in air. This implies that the contribution of hydrogen-environment assistance on FCGR is effectively saturated and further increases in crack growth rates are due to increased stress intensity, as is the case in air. Another way of explaining this change in slope is that at high stress intensities, the crack growth per cycle due to hydrogen assistance outpaces the reach of high hydrogen concentration due to stress, and the contributions from pure fatigue and hydrogen-environment-assisted corrosion are additive.

A second pressure, 34 MPa, was used for measurement of FCGR on these two alloys. As can be seen in Fig. 5, FCGRs seem to increase in general with increasing pressure for the vintage steel, but not for the new steel. FCGR data does converge at values of ΔK greater than 25 MPa·$m^{1/2}$ for both alloys. The new alloy seems to have little pressure dependence, but FCGRs are higher at low pressures, such as 5.5 MPa, than for the vintage alloy. The large-grained ferrite microstructure may play a role in the apparent pressure dependence of the vintage X52 steel.

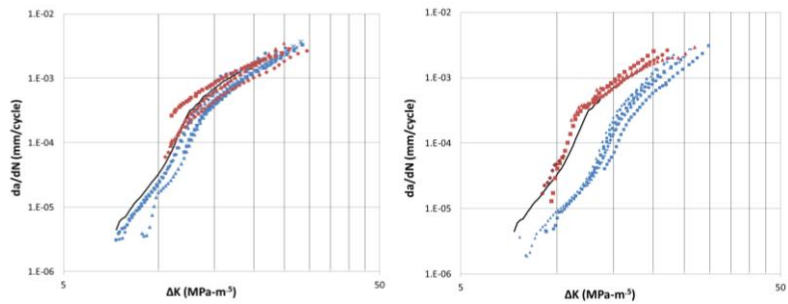

(New) **(Vintage)**

Figure 5. Comparison of FCGR data for two different hydrogen gas pressures, 5.5 MPa (blue) and 34 MPa (red) for the two X52 alloys. SNL data shown for comparison (lines).

CONCLUSIONS

Two X52 steels were measured for FCGR in air, as a baseline, and in pressurized hydrogen gas. The following can be concluded from these data:

- Stage 2 FCGRs for both steels are much higher in hydrogen gas than in air.
- The effect of gas pressure is small, or perhaps nonexistent, for the new X52 steel.
- The effect of gas pressure is larger for the vintage material and occurs more prominently in the stress-enhanced hydrogen diffusion region.
- The older alloy with a ferrite-pearlite microstructure and grain size on the order of 5 µm has a lower FCGR in 5.5 MPa hydrogen than the newer, microalloyed steel with a mixed microstructure of polygonal and acicular ferrite, and a much finer grain size of about 1 µm. The newer steel probably exhibits faster hydrogen diffusion due to microstructure.
- The FCGR curves have a transition, or "knee" around ΔKs of 13 MPa·m$^{1/2}$ and15 MPa·m$^{1/2}$. Before this knee, the increase in FCGR as a function of ΔK is probably due to increasing hydrogen concentration at the crack tip, and after the knee, the hydrogen effect saturates, and further increases in FCGR are attributed to ΔK effects.

ACKNOWLEDGEMENTS

The authors acknowledge James Merritt of the Department of Transportation for his support of this work, and of the Department of Transportation for partial funding of this work under contract DTPH56-09-T-000005. We also acknowledge Lou Hayden and Doug Stalheim for assistance on project planning and microstructural interpretation.

REFERENCES

[1] Fuel cell and hydrogen energy association: transportation, http://www.fchea.org/index.php?id=53 (accessed January 3, 2012).
[2] 2010 Fuel cell technologies market report, June 2011, Department of Energy, http://www1.eere.energy.gov/hydrogenandfuelcells/pdfs/2010_market_report.pdf (accessed January 3, 2012).
[3] Website, August 8, 2012: http://www.freep.com/article/20120807/BUSINESS0104/120807069/Toyota-plans-sell-fuel-cell-car-by-2015
[4] F. Huang, Li, X.G, Liu, J., Qu, Y.M, Jia, J., and Du, C.W., 2011 "Hydrogen-induced cracking susceptibility and hydrogen trapping efficiency of different microstructure X80 pipeline steel," *J. Mater. Sci.* **46**, pp. 715-722.
[5] Mustapha, A., Charles, E.A., Hardie, D., 2012, "Evaluation of environment-assisted cracking susceptibility of a grade X100 pipeline steel," *Corros. Sci.* **54**, pp. 5–9.
[6] Capelle, J., Gilgert, J., and Pluvinage, G., 2010, "A fatigue initiation parameter for gas pipe steel submitted to hydrogen absorption," *Int. J. Hydrogen Energy*, **35**, pp. 833-843.
[7] Alhussein, A., Capelle, J., Gilgert, J., Dominiak, S., and Azari, Z., 2011, "Influence of sandblasting and hydrogen on tensile and fatigue properties of pipeline API 5L X52 steel," *Int. J. Hydrogen Energy*, **36**, pp. 2291-2301.
[8] Cialone, H.J., and Holbrook, J.H., 1988, "Sensitivity of steels to degradation in gaseous hydrogen," *Hydrogen Embrittlment: Prevention and Control, ASTM STP 962*, pp. 134–152.
[9] Nanninga, N.E., Slifka, A.J., Levy, Y.S., and White, C., 2010, "A review of fatigue crack growth for pipeline steels exposed to hydrogen," *J. Res. NIST* **115**, pp. 1–16.

[10] San Marchi, C., Somerday, B.P., Nibur, K., Stalheim, D.G., Boggess, T., and Jansto, S., 2010, "Fracture and fatigue of commercial grade API pipeline steels in gaseous hydrogen," *Proceedings, ASME 2010 Pressure Vessels & Piping Conference*, Bellevue, WA, pp. 1-10.
[11] Lam, P.S., Sindelar, R.L., and Adams, T.M., 2007, "Literature survey of gaseous hydrogen effects on the mechanical properties of carbon and low alloy steels," Proceedings, *ASME 2007 Pressure Vessels & Piping Conference*, San Antonio, TX, pp. 501-518.
[12] Stalheim, D.G., Boggess, T., San Marchi, C., Jansto, S., Somerday, B.P., Muralidharan, G., and Sofronis, P., 2010, "Microstructure and mechanical property performance of commercial API pipeline steels in high pressure gaseous hydrogen," *Proceedings, IPC 2010, 8th International Pipeline Conference,* Calgary, Alberta, Canada, IPC2010-31301.
[13] Suresh, S. and Ritchie, R.O., 1982, "Mechanistic dissimilarities between environmentally influenced fatigue-crack propagation at near-threshold and higher growth rates in lower strength steels," *Metal Science* **16**, pp. 529-538.
[14] Walter, R.J. and Chandler, W.T.,1976, " Cyclic-load crack growth in ASME SA-105 Grade II Steel in high-pressure hydrogen at ambient temperature," *Effect of Hydrogen on Behavior of Materials*, Moran, WY, pp. 273-286.
[15] San Marchi, C., Somerday, B.P., Nibur, K.A., Stalheim, D.G., Boggess, T., and Jansto, S., 2011, "Fracture resisitance and fatigue crack growth of X80 pipeline steel in gaseous hydrogen," *Proceedings, ASME 2011 Pressure Vessels and Piping Conference*, Baltimore, Maryland, PVP2011-57684.
[16] ASME B31.12-2008, "Hydrogen piping and pipelines," American Society of Mechanical Engineers, New York (2009), pp. 258.
[17] ASTM E647-05, "Standard test method for measurement of fatigue crack growth rates," ASTM International, West Conshohocken, PA (2005), pp. 45.
[18] ASTM G142-98, "Standard test method for determination of susceptibility of matals to embrittlement in hydrogen containing environments at high pressure, high temperature, or both," ASTM International, West Conshohocken, PA (2004), pp. 4.
[19] ASTM E8-04, "Standard test method for tension testing of metallic materials," ASTM International, West Conshohocken, PA (2005), pp. 24.
[20] Keller, J., Somerday, B.P., and San Marchi, C., 2012, "Hydrogen embrittlement of structural steels," *FY 2011 Annual Progress Report, DOE Hydrogen and Fuel Cells Program*, pp. 299-302.
[21] Alp, T., Dogan, B., and Davies, T., 1987, "The effect of microstructure in the hydrogen embrittlement of a gas pipe steel," *J. Mater. Sci.* **46**, pp. 2105-2112.
[22] San Marchi, C., Somerday, B.P., Tang, X., and Schiroky, G.H., 2008, "Effects of alloy composition and strain hardening on tensile fracture of hydrogen-precharged type 316 stainless steels," *Int. J. of Hydrogen Energy*, **33**, pp. 889-904.
[23] Lufrano, J. and Sofronis, P.,1998, " Enhanced hydrogen concentrations ahead of rounded notches and cracks – competition between plastic strain and hydrostatic stress," *Acta. Mater*. **46** pp. 1519-1526.